$LiNiPO_4$ Aqueous Rechargeable Battery

Manickam Minakshi[a], David Ralph[a], Mark Blackford[b], and Mihail Ionescu[c]

[a]Department of Chemistry, Murdoch University, Murdoch, WA 6150, AUSTRALIA
[b]Institute of Materials Engineering, ANSTO, Lucas Heights, NSW 2234, AUSTRALIA
[c]Institute for Environment Research, ANSTO, Lucas Heights, NSW 2234, AUSTRALIA

Considering the safety, cost and low ohmic resistance issues with respect to the non-aqueous electrolytes that are generally used in rechargeable lithium ion batteries, aqueous electrolytes attract wide interest. A traditional Zn-MnO_2 battery in which potassium hydroxide (KOH) has been replaced with a lithium hydroxide (LiOH) electrolyte is discussed. As lithium intercalation materials are of special interest as cathode in rechargeable batteries, the new concept has been extended to use lithium nickel phosphate as cathode for aqueous rechargeable batteries. Here, we show reversible extraction and insertion of lithium from and into olivine $LiNiPO_4$ in aqueous solutions. These cells are found to be cheap, rechargeable and safe. The unique sol-gel synthesis has been used to synthesize $LiNiPO_4$ which has been characterized in order to evaluate a new potential cathode for aqueous rechargeable batteries.

Introduction

The demand for the storage of electrical energy has grown both for portable and static applications. As society becomes more and more mobile the demand for a reliable secondary (rechargeable) battery of high energy and power density for a variety of new and existing technologies has increased substantially. In particular, secondary batteries are needed to drive the development of mobile phones, personal computers and power tools. The lithium battery is now the choice for portable electronic devices and is challenging other battery technologies for hybrid vehicle applications. Nevertheless, lithium batteries have been subject to safety concerns caused by overheating following internal short circuits (1). This is due to the reactivity of the battery employing non-aqueous solvents as an electrolyte (2). Lithium electrolytes in ambient atmosphere systems are typically dissolved in organic solvents or polymeric materials and both options limit the battery's performance in comparison with aqueous systems (3). For safety concerns, aqueous electrolytes are the natural choice in the battery field (4-6). Most high-power electrochemical energy storage devices utilize aqueous electrolytes, as they are known to have the highest ionic conductivity. Moreover, aqueous batteries allow higher discharge rates and lower voltage drops due to electrolyte impedance. Hence, a lithium-containing electrolyte might be a candidate for an aqueous rechargeable battery. The key to this approach is the use of an alkaline electrolyte which has high concentrations of Li^+ ions and low concentrations of H^+ ions.

It is widely known that intercalation of lithium or other alkali metal ions into the vacant sites of the oxide or phosphate compounds can be achieved electrochemically in

non-aqueous electrolytes (7-8). The use of aqueous electrolytes is less common because of the reactivity of lithium intercalation compounds with water. There is very limited information on intercalation occurring in aqueous media (5-6, 9-10). If this mechanism is possible in aqueous media these similar host compounds could become rechargeable similar to non-aqueous batteries. Hence it could open up a new field of rechargeable alkaline batteries that utilize oxides or phosphates as the cathode material. To make an attempt, in this study, we have chosen manganese dioxide and lithium transition metal phosphate as a cathode matching with Zn anode and LiOH electrolyte.

The use of manganese dioxide (MnO_2) as the cathode material in Leclanché and alkaline manganese batteries is well known and characterized (11). Primary cells (Leclanché and alkaline) are based on the electrochemical insertion of protons into the host lattice of MnO_2 (12). Under certain conditions the insertion of protons in alkaline cells is reversible (12-13). While intercalation of lithium ions into MnO_2 in non-aqueous electrochemical cells is well known (14-17), there is very limited information on intercalation occurring in aqueous media (5-6, 9-10). This study describes an investigation of the electrochemical behavior of MnO_2 in aqueous LiOH. A particular objective of this study has been to investigate what effect aqueous LiOH has when it is substituted for the traditional potassium hydroxide as the battery electrolyte in alkaline Zn-MnO_2 batteries. The aim was to determine the mechanism through which discharge process of MnO_2 occurs in LiOH as compared to that in KOH and to extend this work in order to evaluate a new lithium intercalation material i.e. $LiNiPO_4$ as cathode in aqueous rechargeable battery.

Since the pioneering work by Padhi et al (18) significant efforts have been made to improve the behavior of olivine-type compounds in organic electrolytes and its application as a cathode in rechargeable lithium battery prototypes (19-20). The information available about the lithium extraction/insertion from/into these compounds in aqueous electrolytes is very scant. In one of our previous publication (21), we have reported the solid state synthesized olivine-type $LiNiPO_4$ and its characterization in aqueous lithium hydroxide (LiOH) electrolyte. However, investigation of olivine compounds in aqueous systems was not widely reported in the literature except our group (9-10, 22). A simple and unique sol-gel process has been used here for the synthesis of $LiNiPO_4$ powder and their electrochemical performance versus Zn anode in LiOH electrolyte is reported for the first time. The aqueous rechargeable battery has resulted in patentable technology at Murdoch University (22). The proposed aqueous rechargeable battery offers immediate advantages over existing battery technologies with respect to cost, safety and environmental considerations.

Experimental

Material Synthesis

The EMD (electrolytic manganese dioxide; γ-MnO_2) type (IBA sample 32) used in this work was purchased from the Kerr McGee Chemical Corporation. Bismuth oxide (Bi_2O_3) was obtained from Aldrich chemical company. A sol-gel method is used to prepare $LiNiPO_4$/C composites cathode material in our laboratory. $LiNiPO_4$ powders were synthesized from stoichiometric ratio of the precursors containing lithium acetate ($LiOOCCH_3.2H_2O$), nickel acetate $(CH_3COO)_2Ni.4H_2O$ and di hydrogen ammonium

phosphate ($NH_4H_2PO_4$) and citric acid. The mixtures of equal molars of precursors were dissolved in an aqueous solution of citric acid. The resulting solution was continuously stirred at 80^{o}C until it changed to gel. Subsequently, the gel was first dried at 110^{o}C for 12 h in air and then calcined at 550^{o}C for 10 h in air with intermittent grindings. The synthesized products were ground with a mortar and pestle to powder for microstructural characterization and electrochemical testing.

Electrochemical characterization

Galvanostatic discharge/charge of Zn/MnO_2 (or) $LiNiPO_4$ –aq. LiOH cell

The MnO_2 active material was first mixed with 15 wt.% of carbon black (A-99, Asbury USA) and with 10 wt.% of poly(vinylidene difluoride) (PVDF, Sigma Aldrich) as a binder and then pressed into a disc shape with a diameter of 12 mm. Each disk was 0.5 mm thick and weighed approximately 20 mg. An electrochemical test cell was fabricated with the disk as the cathode, Zn metal as the anode (with identical dimensions to the cathode) and filter paper (Whatman filters) as the separator. The electrolyte was a saturated solution of lithium hydroxide containing 1 mol L^{-1} zinc sulphate. Analytical reagent grade zinc sulphate heptahydrate ($ZnSO_4 \cdot 7H_2O$), lithium hydroxide monohydrate ($LiOH \cdot H_2O$) and potassium hydroxide (KOH) were dissolved in de-ionized water to prepare solutions of required concentrations. The cells were charged/discharged galvanostatically at 0.2 mA by using an 8 channel battery analyser from Shenzhen Neware Technology Company, China, operated by a battery testing system (BTS). The charge and discharge cut-off voltage were of 1.9 and 0.5 V respectively. All electrochemical measurements were carried out at ambient temperature (25 ± 1^o C).

Slow-scan cyclic voltammetric investigation of $LiNiPO_4$

For cyclic voltammetric (CV) experiments, a standard three-electrode cell was used. For this purpose, the $LiNiPO_4$ working electrode was made as follows: $LiNiPO_4$ powder was pressed on to a disc of Pt gauze. On the other side of a disc, a layer of conductive carbon (A-99, Asbury USA) was also pressed. The $LiNiPO_4$ side of the disc was exposed with a hole of 1 mm to the LiOH electrolyte through a Teflon barrel. For making electrical connection of the working electrode a Pt disc was inserted into the barrel on top of the carbon side which contacted a stainless steel plunger. The counter electrode was a zinc foil, which was separated from the main electrolyte by means of a porous frit. A saturated Hg/HgO (from Koslow Scientific) served as the reference electrode. Reported potentials are relative to Hg/HgO. The electrolyte was saturated aqueous lithium hydroxide. The working electrode was cycled between 0.2 and –0.3 V at 25 μV /s scan rate. An EG&G Princeton Applied Research Versa Stat III model was used to scan the potential. On each occasion the potential scan started at -0.3 V, moving initially in the anodic direction.

Physical characterization of the materials

The experimental details of sample preparation for various physical characterizations methods were similar to those reported earlier (9-10, 21). For X-ray analysis a Siemens X-ray diffractometer using Philips Cu-Kα radiation was used. Transmission electron microscopy (TEM) was performed using a JEOL JEM 2010F (JEOL, Japan) equipped with a field emission gun (FEG) electron source operated at 200kV. The morphology of the as-synthesized $LiNiPO_4$ material was characterized by TEM. Phase and structure of the material were monitored using selected area diffraction (SAD). TEM specimens were prepared by scraping a small fragment from the pressed pellet, lightly grinding under

ethanol and dispersing on-to a holey carbon support film. Specimens were examined at liquid nitrogen temperature in a cooling stage, to reduce beam damage and contamination effects. The surface analysis of the materials was conducted by using a scanning electron microscope (Philips Analytical XL series 20).

Results and Discussion

Electrochemical behavior of MnO_2 in Zn/MnO_2 – aqueous potassium hydroxide (KOH) cell

The cell characteristics of Zn/MnO_2 using a 7 M KOH as the electrolyte were investigated. The cell was galvanostatically discharged first and then attempted to charge at the same current density. The results are shown in Fig.1a. During the discharge process, shape of the curve is characterized by an initial drop in voltage (from 1.55 to 1.5 V) followed by a gradual decrease in potential to the discharge cut-off voltage of 1.0 V. A plateau of the cell voltage is seen in the discharge curve until 1.35 V. The discharge capacity of ca. 250 mAh/g was obtained per gram of MnO_2 mass for 0.2 mA constant discharge current. The sharp drop in discharge voltage (from 1.2 to 1.0 V) in Fig. 1a, shows that the cell is limited by Zn anode (23). During subsequent charge, the battery is found to be not rechargeable. In one of our recent work (24) we explained that redox mechanism involved in this cell is a K^+ ion insertion on the host MnO_2 and this process is irreversible. The K^+ ion from the electrolyte into the cathode retard the usual protonation mechanism (25) for reversibility. The cell reversibility also depends on the different concentrations of KOH. Many attempts have been made to make this alkaline Zn-MnO_2 cell rechargeable, and reported that by physical admixture of bismuth oxide the MnO_2 cathode cell could be rechargeable (26-27). In accordance with this, we assessed the influence of Bi_2O_3 additives on the rechargeability of Zn/MnO_2 battery.

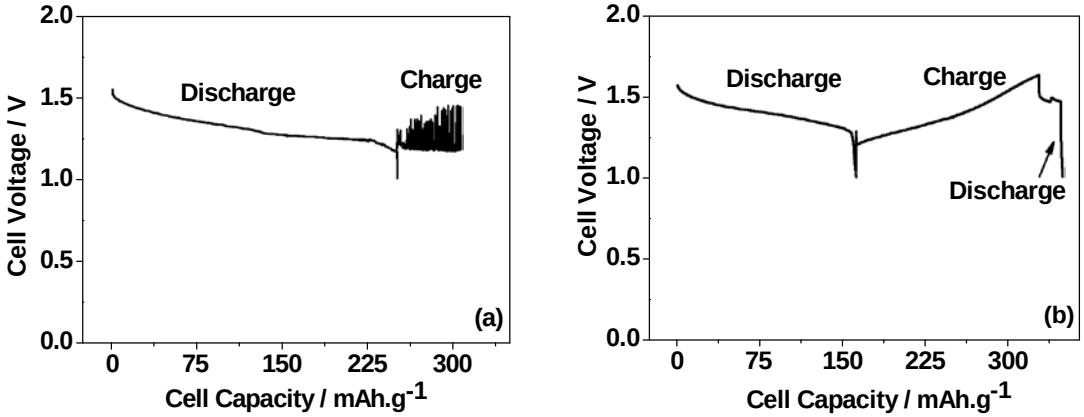

Figure 1. Discharge-charge curves illustrating the cyclability of Zn/MnO_2 cells (a) additive free MnO_2 and (b) Bi_2O_3 (5 wt.%) added MnO_2. Both the cells contain 7 M concentration of aqueous KOH as the electrolyte.

The discharge-charge voltage profiles of the bismuth-doped MnO_2 cathode are shown in Fig. 1b. The Bi-containing MnO_2 cell shows slightly higher discharge voltage but the capacity is limited to ca. 160 mAh/g against 250 mAh/g (for the Bi free cathode in Fig. 1a). The striking difference for the Bi-containing cell is fully rechargeable. It is claimed

(28) bismuth additive play a preventive role in the formation of Mn_3O_4 product and stabilizes the host MnO_2 structure. However, the cell is not rechargeable for the successive cycles as seen in Fig. 1b. Attempts to produce a viable Zn/MnO_2 secondary battery have failed owing primarily to the highly irreversible behavior of MnO_2 electrode, limiting the life of the battery. Hence, presently, the commercial use of Zn/MnO_2 system is limited to primary batteries.

Electrochemical behavior of MnO_2 in Zn/MnO_2 – aqueous lithium hydroxide (LiOH) cell

In accordance with the objective of this study, the effect of replacing KOH with LiOH was determined by carrying out a discharge-charge cycles on a Zn/MnO_2 cell containing LiOH electrolyte. The results for the first cycle are shown in Fig. 2a. The discharge characteristics and the capacity are quite identical to that of Fig. 1b but the increase in cell potential during charge was higher when LiOH was the electrolyte. Figure 2b shows the reversibility of the Zn/MnO_2 with LiOH electrolyte. The cell could be reversibly discharged for multiple cycles. Notably, a new class of rechargeable manganese dioxide electrode is reported for the first time using LiOH as the electrolyte. The zinc-manganese dioxide ($Zn\text{-}MnO_2$) battery had a capacity of 150, 130 and 105 mAh/g at 1st, 50th and 100th cycle (29). This corresponded to a loss in efficiency of just 30% after multiple cycles. Hence, the commercial alkaline $Zn\text{-}MnO_2$ primary battery has been transformed into a secondary battery using LiOH electrolyte. Further improvement in the cyclability of this cell is investigated and reported by us (30-31).

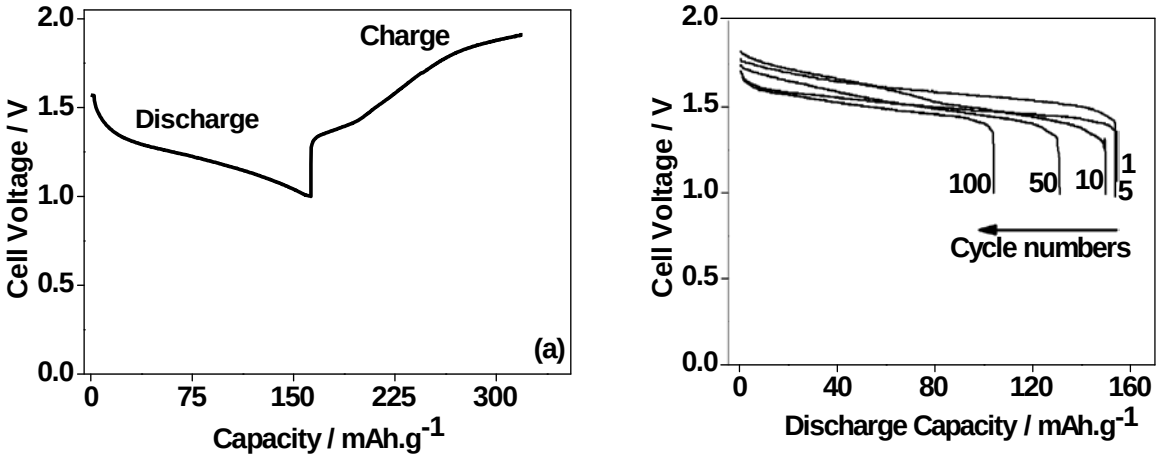

Figure 2. Discharge-charge curves illustrating the cyclability of Zn/MnO_2 cells (a) first cycle and (b) subsequent cycles. Both the cells contain saturated concentration of aqueous LiOH containing 1 mol L^{-1} of $ZnSO_4$ as the electrolyte. Cycle numbers are indicated in the figure.

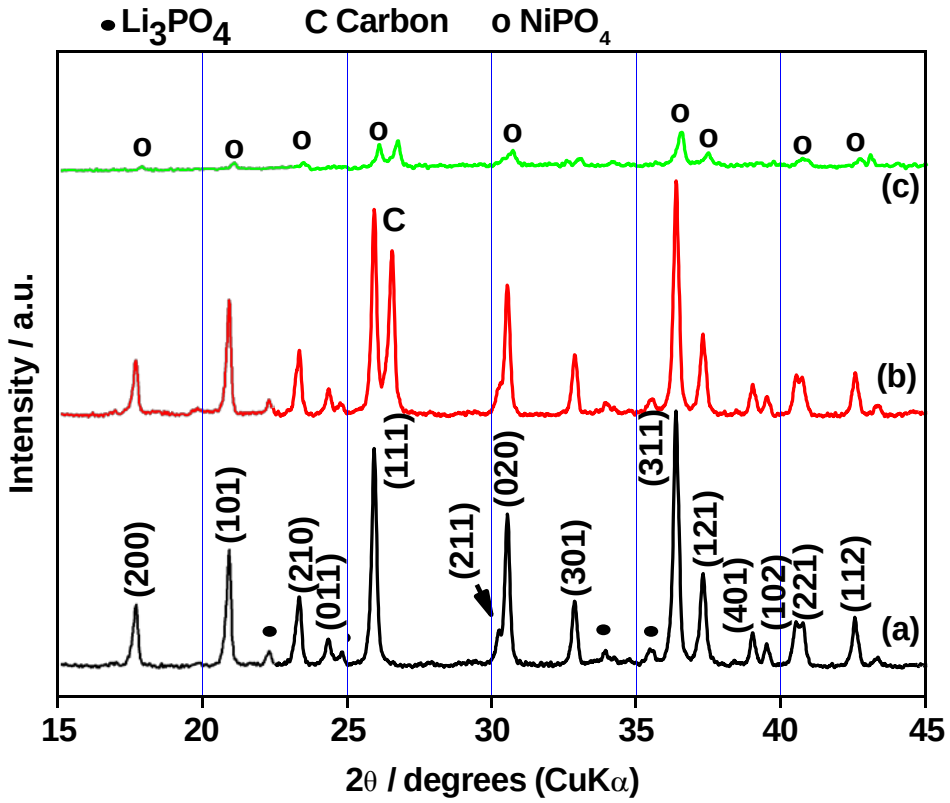

Figure 3. XRD patterns of $LiNiPO_4$ olivine (a) as-synthesized, (b) before and (c) after charged. Lines are indexed in the orthorhombic system. Li_3PO_4 (●) is identified as a second phase. **Fig. 3c** shows the pattern for the electrode after oxidation in aqueous LiOH electrolyte. "O" corresponds to (delithiated) $NiPO_4$ peaks.

This new concept with excellent results motivated a search for other potential cathodes suitable for aqueous rechargeable batteries which might be suitable for use as battery cathodes.

Electrochemical behavior of olivine type $LiNiPO_4$ in Zn/$LiNiPO_4$ – aqueous lithium hydroxide (LiOH) cell

Another major objective of this paper is to establish whether olivine type lithium nickel phosphate could be used as a cathode in aqueous battery. The focus of this work is on establishing the mechanism through which electro-oxidation of this material occurs in aqueous LiOH electrolyte and how it compares with that known for the same in non-aqueous electrolytes. The material $LiNiPO_4$ was prepared through unique sol-gel process (32-33) in order to achieve products with high purity, homogeneity, dispersive grains of small size and the lower processing temperature compared with conventional ceramic powder methods. The X-ray diffraction pattern of the $LiNiPO_4$ as-synthesized material is shown in Fig. 3a. The miller indices (h k l) of the diffraction peaks are indexed in Fig. 3a. The important characteristic of the XRD spectrum is that all the major peaks are well assigned to $LiNiPO_4$ phase with a minor phase of Li_3PO_4 as an impurity.

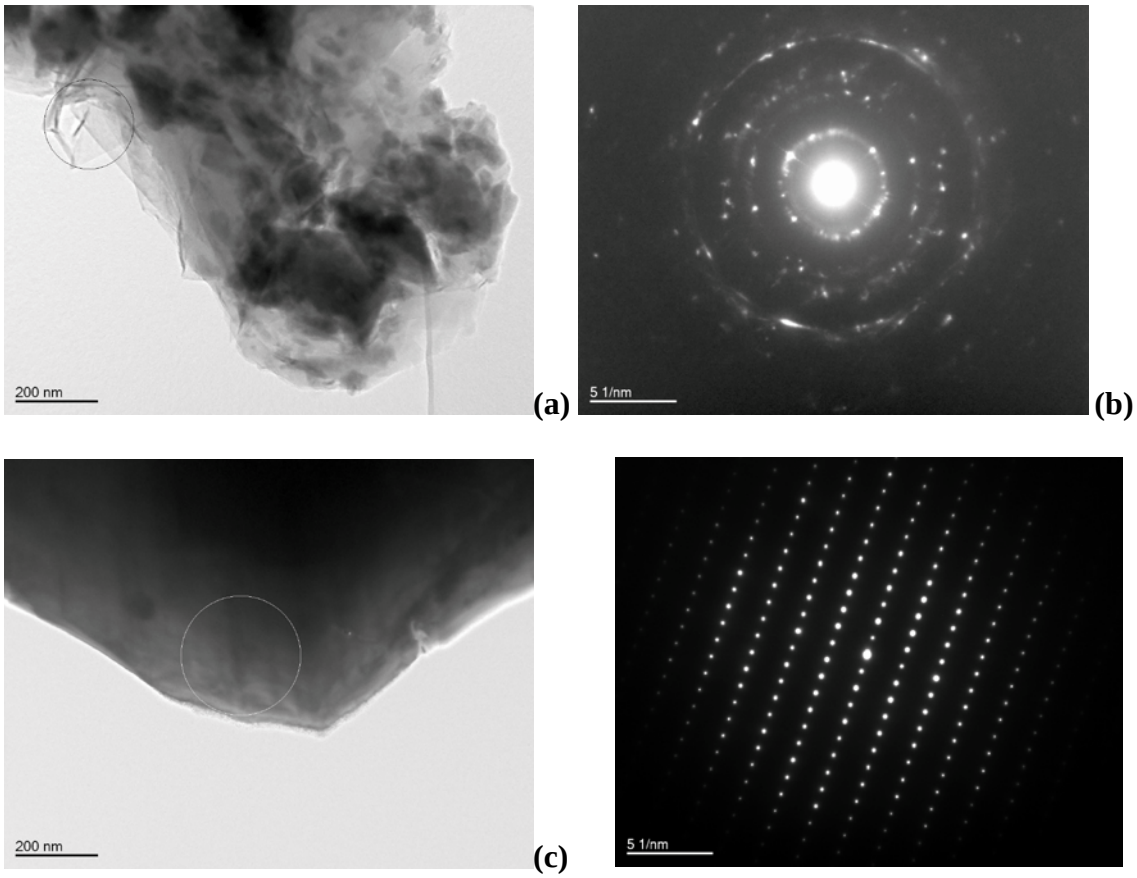

Figure 4. TEM images and selected area diffraction patterns (SADP) of the as-prepared olivine $LiNiPO_4$. Fig. 4a shows carbon (confirmed by EDS) coated / wrapped on the cathode material. Fig. 4b is the SADP from the circled area in Fig. 4a confirming the structure is crystalline graphite. Fig. 4c shows a discrete $LiNiPO_4$ particle. Fig. 4d is the SADP from the circled area in Fig. 4c showing the structure is highly crystalline.

Morphological characterization of the as-synthesized $LiNiPO_4$ was carried out by transmission electron microscopy (TEM), energy dispersive x-ray spectroscopy (EDS) and selected area diffraction (SAD). Much of the $LiNiPO_4$ material was found to be encapsulated in carbon (Fig. 4a) and SADP analysis showed this to be crystalline graphite. Particle size ranged from a few hundred nanometers to several microns, and the surface of particles was often coated with thin carbon layers that reinforce the internal contact of $LiNiPO_4$. It is understood that citric acid (chosen as chelating agent) acts as a carbon source (34) that enhanced the electronic conductivity of the composite. The in-situ carbon coating on the phosphate material can lead to better inter-particle contacts and improved diffusion of lithium-ions. Hence, it is an effective way to improve the rate capability of $LiNiPO_4$. SADP analysis (Fig 4b and 4d) from the circled locations shown in Fig. 4a and 4c confirms the crystalline structure of carbon and $LiNiPO_4$, respectively.

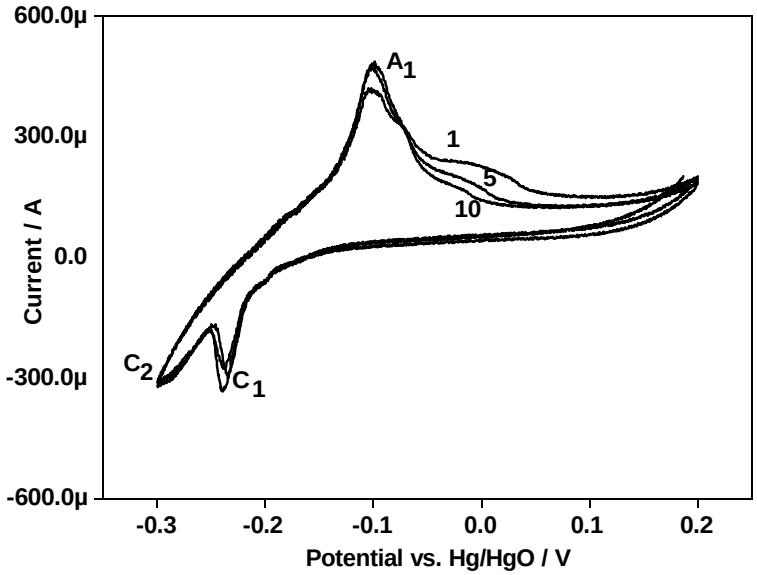

Figure 5. A typical cyclic voltammogram of lithium nickel phosphate ($LiNiPO_4$) in aqueous lithium hydroxide electrolyte (scan rate: 25 µV. s^{-1}; potential limit: 0.2 to -0.3 V and back). Cycle numbers are indicated in the figure.

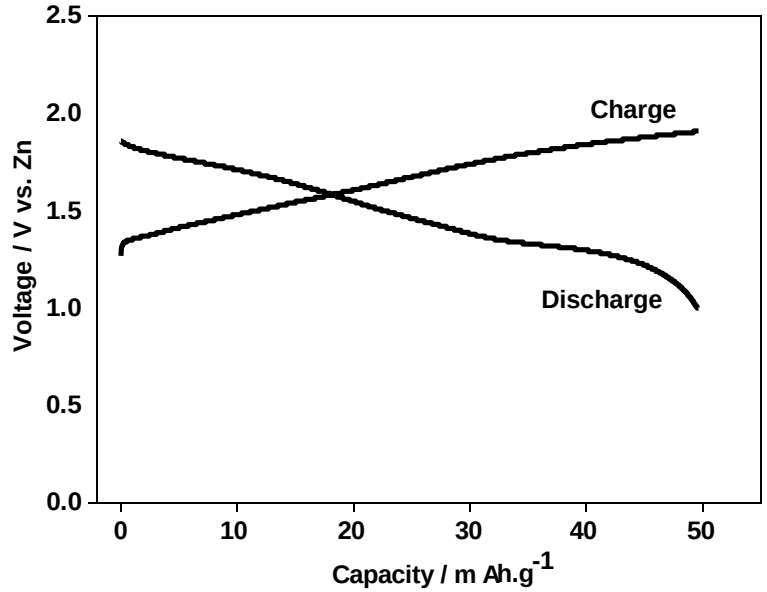

Figure 6. Typical galvanostatic (charge-discharge) curves for annealed olivine $LiNiPO_4$ in aqueous LiOH electrolyte at a current density of 0.5 mA/cm^2. Metallic Sn is used as an anode.

To investigate the oxidation-reduction reactions of Ni^{3+}/Ni^{2+}, cyclic voltammetry and galvanostatic discharge/charge tests were undertaken. Figure 5 shows a typical cyclic voltammogram of $LiNiPO_4$. The scan was initiated at -0.3 V going in the anodic direction

to +0.2 V and then reversing it to the starting potential. The material exhibits a distinct oxidation peak A_1 at -99 mV and a corresponding small reduction peak C_1 at -237 mV. The peak due to hydrogen evolution is also seen in Fig. 5, indicated as C_2 at -295 mV. It shows that the redox reaction involves a one-stage process of oxidation and reduction processes. To evaluate the practical application of this material, the cell was galvanostatically charged and then discharged at the same current density. The first discharge-charge curves are shown in Fig. 6. During the charge process there was a gradual increase in potential to the charge cut-off voltage of 1.8 V. During discharge, there was a gradual decline in potential till 1.3 V and which it dropped rapidly to the cut-off voltage of 1.0 V. The columbic efficiency of the charge-discharge process was ca. to be approximately 95% and the available capacity was 50 mAh/g. This excellent efficiency can be attributed to the homogeneity of the material and improvement of electrical conductivity via in-situ carbon coating. Long term cycling behavior of the $LiNiPO_4$ cathode is shown in Fig. 7. The discharge capacities are quite constant and it was 49 mAh/g after the 50^{th} cycle and there is a loss of only 2% from the initial capacity.

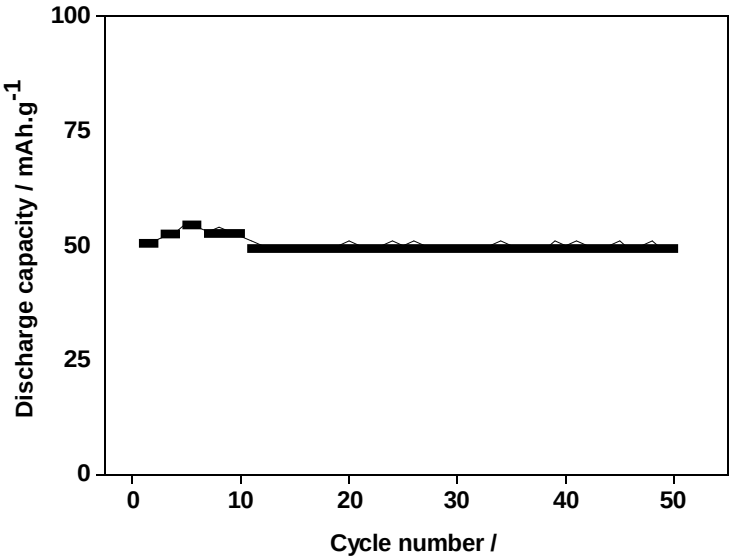

Figure 7. Cyclability of Zn-$LiNiPO_4$ battery using LiOH electrolyte

To determine the mechanism through which $LiNiPO_4$ undergoes electron transfer reactions in aqueous solutions, the X-ray diffraction analysis were carried out on the starting material $LiNiPO_4$ and those of the products formed on its electro-oxidation are shown in Figs 3b-c. The XRD pattern of the $LiNiPO_4$ cathode mixed with carbon for conductivity before any electrochemical treatment is shown in Fig. 3b. The pattern indicates that the material $LiNiPO_4$ was crystalline of orthorhombic structure. The product of the material formed on electro-oxidation (Fig. 3c) showed that the observed peaks are lower in intensity and shifted to lower 2 theta values comparing to that of in Fig. 3b. The emergence of these new peaks (o) is assumed to be lithium extracted $NiPO_4$ as there are no consistent literature data for comparison. Thus the oxidation of $LiNiPO_4$ in aqueous LiOH involves de-intercalation of Li^+ and hence the mechanism resembles that in non-aqueous solvents reported for other olivine compounds i.e. Li*M*PO_4 (*M*=Co, Fe or Mn). Elastic recoil detection analysis (ERDA) analysis (not given here) support the XRD data that the concentration of lithium in the bulk material was much lower for the charged

sample, indicating that lithium is extracted from the $LiNiPO_4$ during charge process. This is in contrast to our report published earlier (35) on the material synthesized through solid-state reaction, there we have seen delithiated $NiPO_4$ along with the formation of NiOOH as the products after electro-oxidation. This implies that citric acid added sol-gel method for the synthesis of $LiNiPO_4$ powder improved the active particles with a maximum concentration of lithium ion diffusion during battery discharge/charge. This unique synthesis method with a smaller in particle size (Fig. 8a) proved favorable for the intercalation/de-intercalation of lithium-ion process and the primary particles appears to be agglomerated for the charged material as seen in Fig. 8b. Hence, the high potential in sol-gel synthesized $LiNiPO_4$ looks to be very attractive in terms of high energy density, given the capacity is improved.

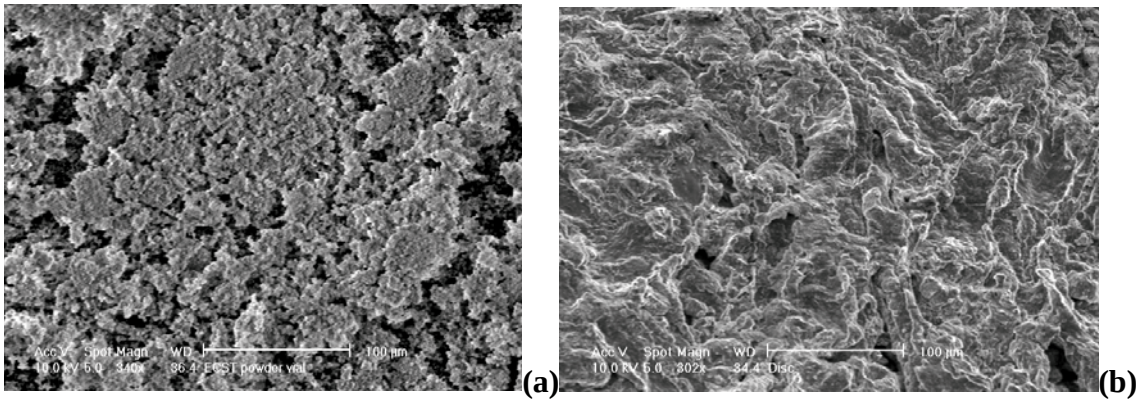

(a) **(b)**

Figure 8. Scanning electron micrographs of $LiNiPO_4$ olivine (a) before and (b) after charging. The shape and size of the primary $LiNiPO_4$ particles appears to be agglomerated after charging.

Conclusion

The proposed aqueous rechargeable battery (Zn-MnO_2 and Zn-$LiNiPO_4$) in aqueous LiOH electrolyte offers immediate advantages over existing battery technologies with respect to cost, safety and environmental considerations. The aqueous rechargeable cell has several advantages such as (a) high ionic conductivity so thick electrodes can be used (b) expensive lithium salts ($LiPF_6$ + Ethylene carbonate: Propylene carbonate) have been replaced by cheap LiOH as electrolyte (c) improved columbic efficiency and (d) safety issues are solved with stringent cell assembly in protective glove box atmosphere is not required. However, it will be necessary to improve the power density and test long term cycle life in order to make this technology competitive with the performance of current Li-based battery systems.

The battery with LiOH electrolyte functions quite differently from the traditional cell, which uses KOH cell. When a cell containing aqueous LiOH is discharged in Zn-MnO_2, lithium is intercalated into the MnO_2 structure and the process is reversible for multiple cycles. K^+ ion intercalation is not reversible in KOH cell. The preliminary results for the Zn-$LiNiPO_4$ cell show that the citric acid added sol-gel method is a unique technique to prepare $LiNiPO_4$ composites with an improved electrochemical performance and the charge/discharge mechanism is quite similar to that reported for non-aqueous solvents.

Acknowledgements

The author (M. M) wishes to acknowledge the Australian Research Council (ARC). This research was supported under ARC's Discovery Projects funding scheme (DP1092543). The views expressed herein are those of the authors and are not necessarily those of the Australian Research Council. CASS foundation is greatly acknowledged by (M. M) for providing a travel grant to attend the 219th ECS Meeting at Montreal, QC, Canada.

References

1. T.M. Florence and Y. T. Farrar, Anal. Chem., **40**, 1200 (1968).
2. P.G. Balakrishnan, R. Ramesh and T. Prem Kumar, J. Power Sources, **155,** 401 (2006).
3. K. Amine, H. Yasuda and M. Yamachi, Electrochem. Solid-State Lett., **3**, 178 (2000).
4. F. Beck and P. Ruetschi, Electrochim. Acta, **45,** 2467 (2000).
5. R.L. Deutscher, T.M. Florence and R. Woods, J. Power Sources, **55,** 41 (1995).
6. R. Ruffo, C. Wessells, R.A. Huggins and Y. Cui, Electrochem. Commun., **11**, 247 (2009).
7. S. Bach, J.P.P. Ramos, N. Baffier and R. Messina, Electrochim. Acta., **36**, 1595 (1991).
8. E. Levi, E. Zingrad, H. Teller, M.D. Levi, D. Aurbach, E.Mengeritsky, E. Elster, P. Dan, E.Granot and H. Yamin, J. Electrochem. Soc., **144**, 4133 (1977).
9. M. Minakshi, P. Singh, T. B. Issa, S. Thurgate and R. DeMarco, J. Power Sources, **130**, 254 (2004).
10. M. Minakshi, P. Singh and D. R.G. Mitchell, J. Electrochem. Soc., **154**, A109 (2007).
11. F.L. Tye in Electrochemical Power Sources, M. Barak, Editor, p. 50, Peter Peregrinus, London (1980).
12. C. Mondoloini, M. Laborde, J. Rioux, E. Andoni and C. Levy-Clement, J. Electrochem. Soc., **139**, 954 (1992).
13. Scott W. Donne, Geoffrey A. Lawrence, and Dom A.J. Swinkels, J. Electrochem. Soc., **144**, 2949 (1997).
14. H. Ikeda, J. Power Sources, **9**, 329 (1983).
15. G. Pistoia, J. Electrochem. Soc., **129**, 1861 (1982).
16. F. Fillaux, C.H. Cachet, H. Ouboumour, J. Tomkinson, C. Levy-Clement and L.T. Yu, J. Electrochem.Soc., **140**, 585 (1993).
17. T. Ohzuku, M. Kitagawa and T. Hirai, J. Electrochem. Soc., **136**, 3169 (1989).
18. A. K. Padhi, K.S. Nanjundaswamy, C. Masquelier, S. Okada and J.B. Goodenough, J. Electrochem. Soc., **144**, 1188 (1997).
19. T. Muraliganth and A. Manthiram, J. Phys. Chem. C., **114,** 15530 (2010).
20. N. N. Bramnik, K. Nikolowski, C. Baehtz, K. G. Bramnik and H. Ehrenberg, Chem. Mater., **19,** 908 (2007).
21. M. Minakshi, P. Singh, D. Appadoo and D. Martin, Electrochim. Acta **56,** 4356 (2011).
22. M. Minakshi, PCT Int. /WO 2011/044644.
23. M. Minakshi, D. Appadoo and D. Martin, Electrochem. Solid State Lett., **13** A77 (2010).

24. M. Minakshi, J. Electroanal. Chem., **616**, 99 (2008).
25. J. McBreen, Electrochim. Acta, **20**, 221 (1975).
26. K. Kordesch, J. Gsellmann, M. Peri, K. Tomantschger and R. Chemelli, Electrochim. Acta, **26**, 1495 (1981).
27. H. S. Wroblowa and N. Gupta, J. Electroanal. Chem., **238**, 93 (1987).
28. D. Im and A. Manthiram, J. Electrochem. Soc., **150**, A68 (2003).
29. M. Minakshi and D. R. G. Mitchell, Electrochim. Acta, **53,** 6323 (2008).
30. M. Minakshi, D. R. G. Mitchell and K. Prince, Solid State Ionics, **179,** 355 (2008).
31. M. Minakshi and M. Blackford, J. Alloys Compd., **509**, 5974 (2011).
32. L. J. Fu, H. Liu, C. Li, Y.P.Wu, E. Rahm, R. Holze and H.Q. Wu, Prog. Mater. Sci., **50**, 881 (2005).
33. Y.Q. Hu, M. M. Doeff, R. Kostecki and R. Finones, J. Electrochem. Soc., **151**, A1279 (2004).
34. Z. H. Chen and J. R. Dahn, J. Electrochem. Soc., **149**, A1184 (2002).
35. M. Minakshi, P. Singh, D. Appadoo and D. Martin, Electrochim. Acta **56,** 4356 (2011).